

Electronic Supplementary Information (ESI)

Rapid template free synthesis of nanostructured conducting polymer film by tuning morphology using hyperbranched polymer additive

Chun-Fu Lu, Song-Fu Liao, Ke-Hsin Wang, Chin-Ti Chen, Chi-Yang Chao and Wei-Fang Su*

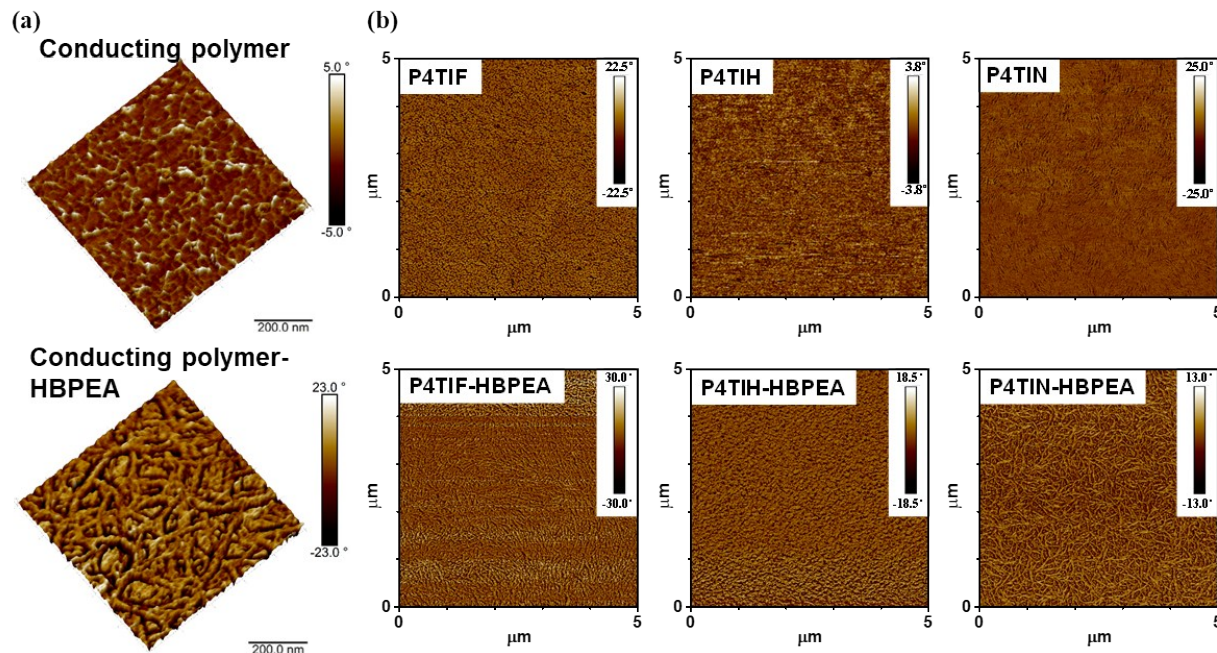


Figure S1. (a) AFM phase images of polymer film and conducting polymer-HBPEA film. (b) AFM phase images of neat polymer film (P4TIF, P4TIH and P4TIN) and CP-HBPEA film (P4TIF-HBPEA, P4TIH-HBPEA and P4TIN-HBPEA).

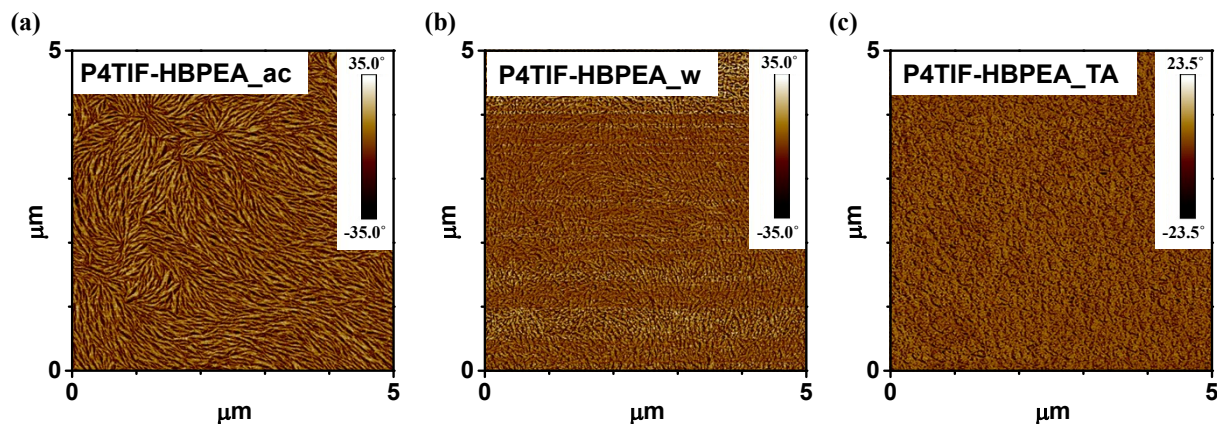


Figure S2. AFM phase images of a) P4TIF-HBPEA_ac; b) P4TIF-HBPEA_w and c) P4TIF-HBPEA_TA.

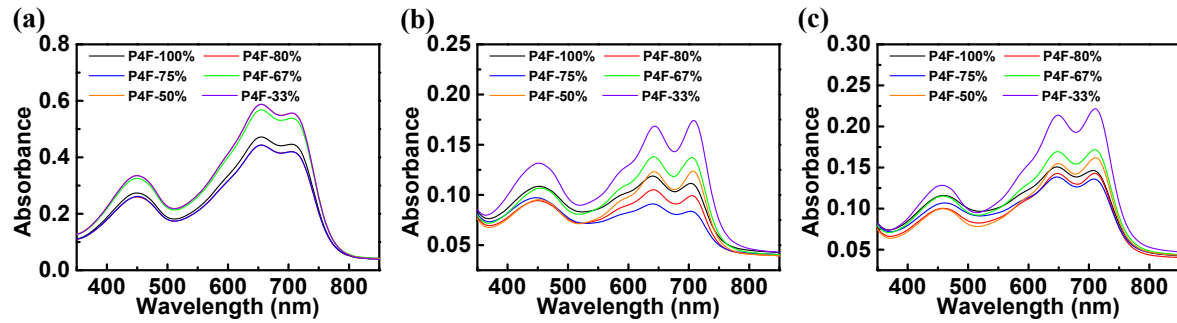


Figure S3. The UV-vis spectra of (a) P4TIF-HBPEA chloroform solution; (b) P4TIF-HBPEA_ac films and (c) P4TIF-HBPEA_TA films.

Table S1. Vibrational peaks of P4TIF in P4TIF-HBPEA blends characterized by UV-vis absorption spectra.

Sample	Solution λ_{0-0} [nm]	λ_{0-1} [nm]	As-cast film λ_{0-0} [nm]	λ_{0-1} [nm]	Thermal annealed film λ_{0-0} [nm]	λ_{0-1} [nm]
P4F-100%	705	655	707	648	703	640
P4F-80%	705	655	710	648	705	642
P4F-75%	705	655	710	648	703	641
P4F-67%	705	655	710	649	705	642
P4F-50%	705	655	710	649	707	643
P4F-33%	705	655	710	649	708	643

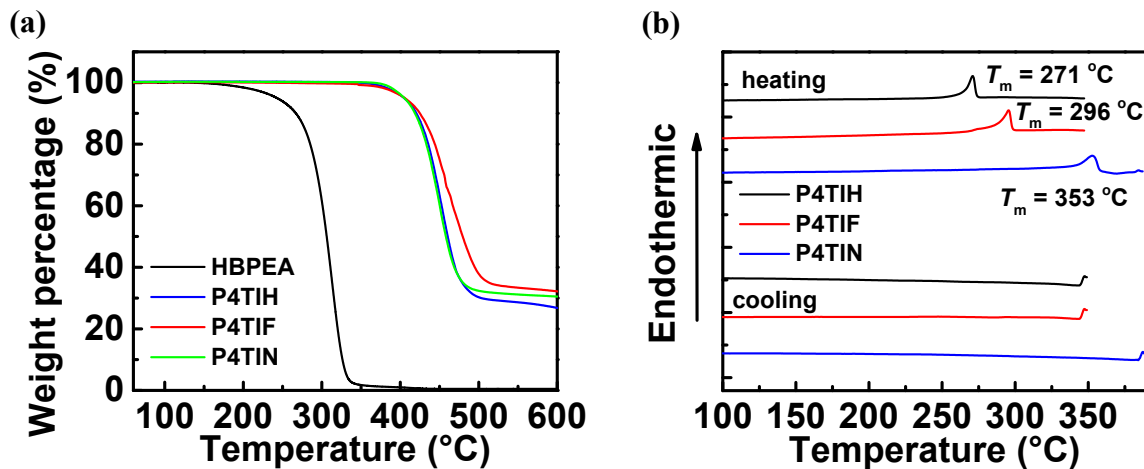


Figure S4. (a) TGA thermograms of HBPEA, P4TIH, P4TIF and P4TIN; (b) DSC thermograms of P4TIH, P4TIF and P4TIN.

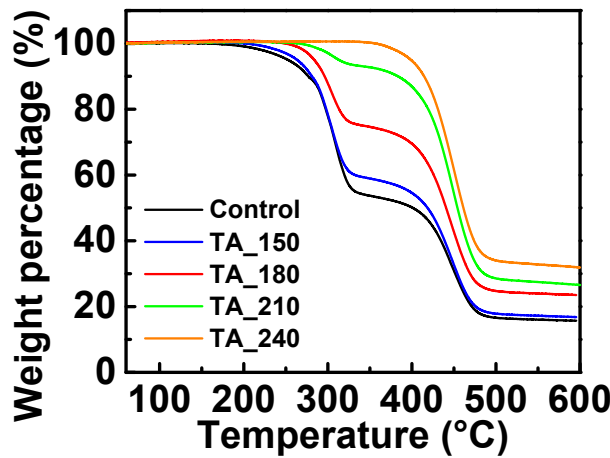


Figure S5. TGA thermograms of P4TIF-HBPEA bulk materials with thermal treatment at 150, 180, 210 and 240°C.

Table S2. P4TIF content in P4TIF-HBPEA bulk materials with thermal treatment at 150, 180, 210 and 240°C.

Sample	P4TIF content [wt%] ^{a)}
Control	53.6
TA_150	58.8
TA_180	74.5
TA_210	92.7
TA_240	100

^{a)} The composition of P4TIF is determined by TGA

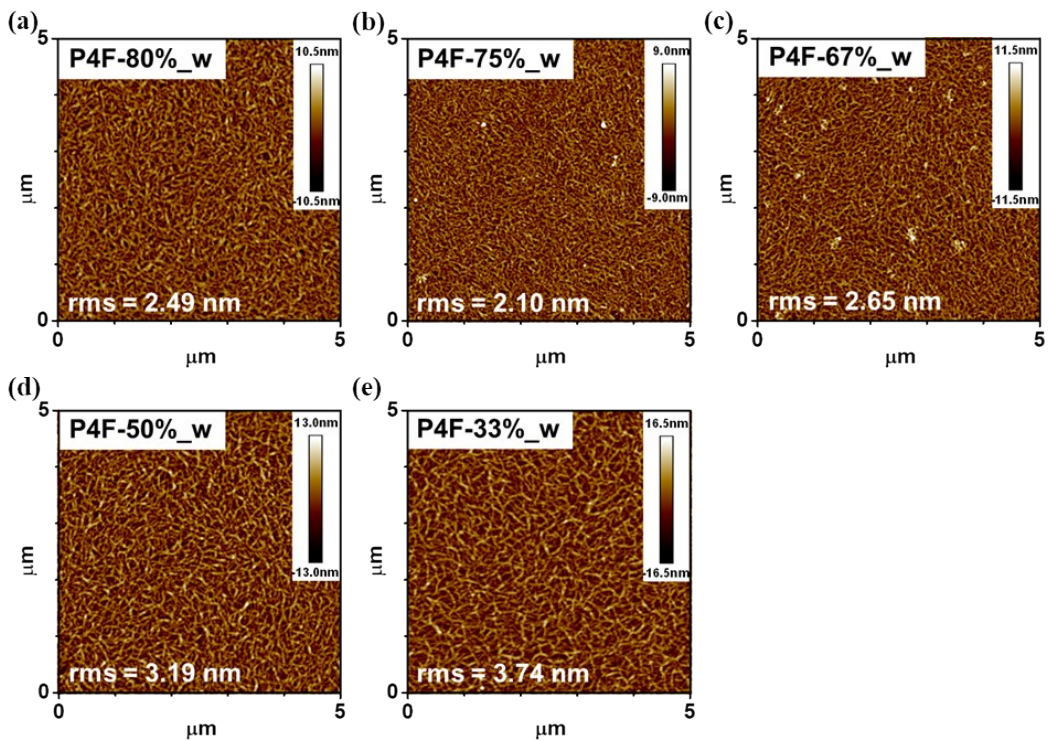


Figure S6. The AFM topographic images of (a) P4F-80%_W, (b) P4F-75%_W, (c) P4F-67%_W, (d) P4F-50%_W and (e) P4F-33%_W.

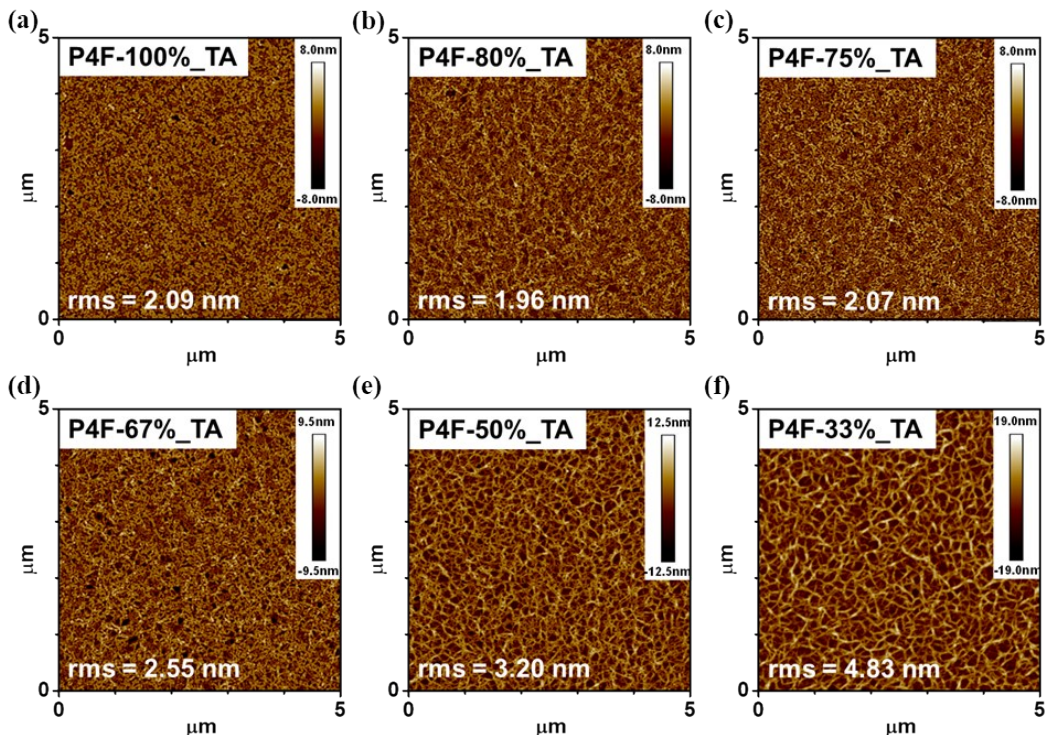


Figure S7. The AFM topographic images of (a) P4F-100%_TA, (b) P4F-80%_TA, (c) P4F-75%_TA, (d) P4F-67%_TA, (e) P4F-50%_TA and (f) P4F-33%_TA.

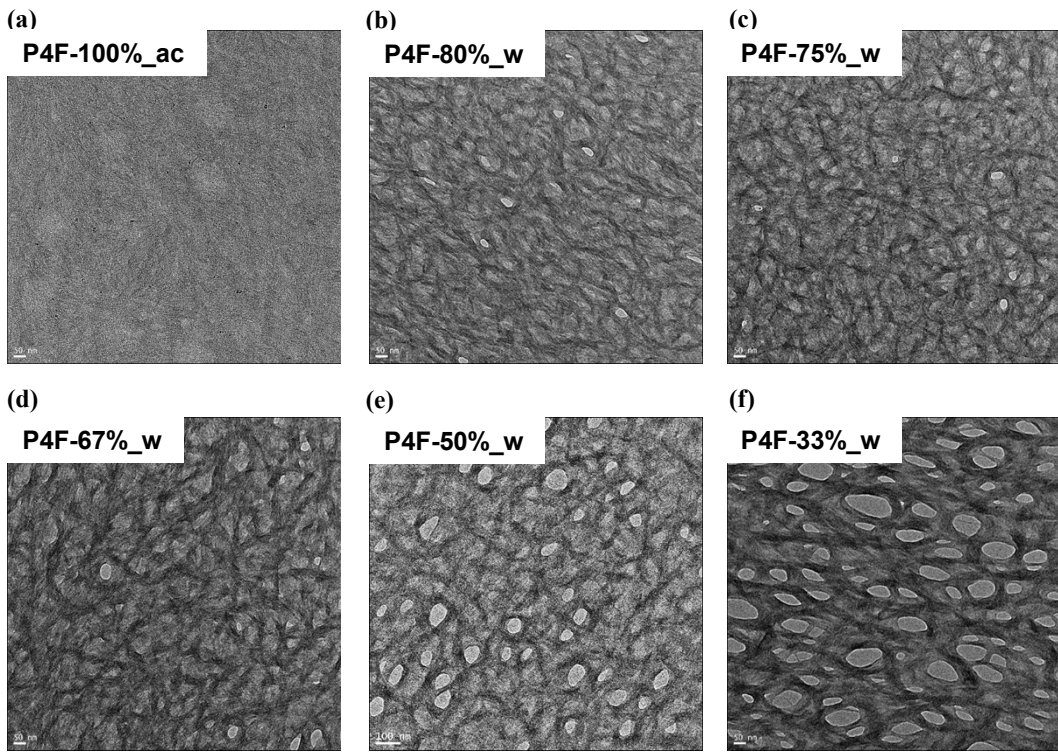


Figure S8. The TEM images of (a) P4F-100%_ac, (b) P4F-80%_w, (c) P4F-75%_w, (d) P4F-67%_w, (e) P4F-50%_w and (f) P4F-33%_w.

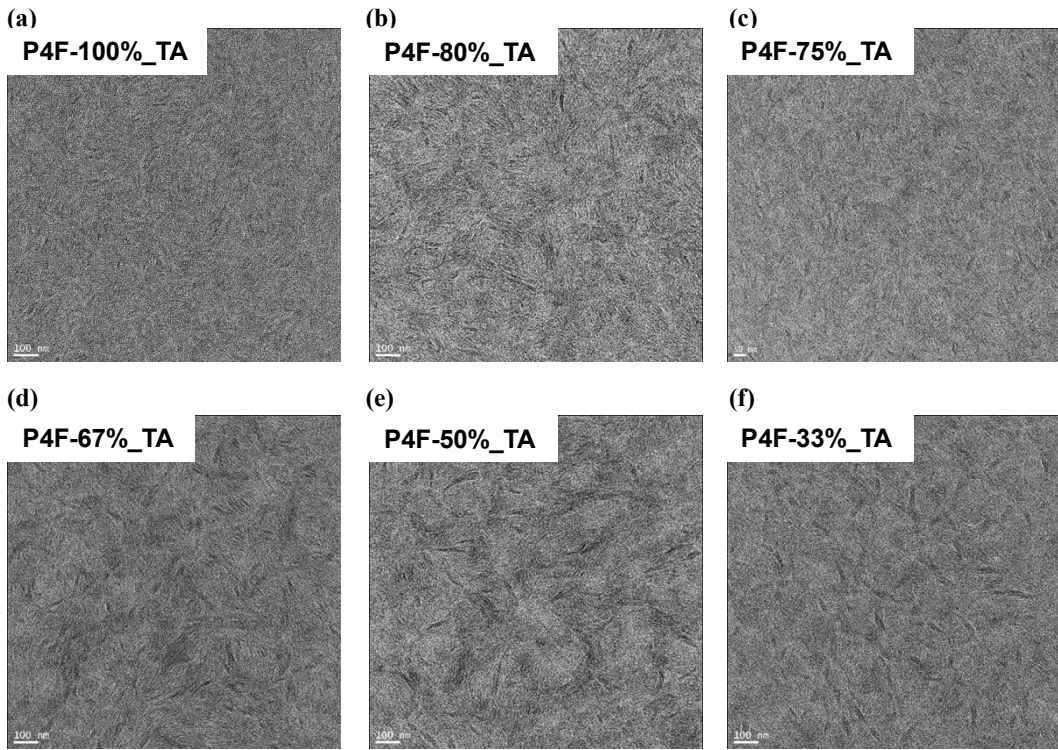


Figure S9. The TEM images of (a) P4F-100%_TA, (b) P4F-80%_TA, (c) P4F-75%_TA, (d) P4F-67%_TA, (e) P4F-50%_TA and (f) P4F-33%_TA.

Table S3. Electrical properties of neat P4TIX films after thermal annealing.

Sample	$\mu_{\text{sat}} [\text{cm}^2\text{V}^{-1}\text{s}^{-1}]$	on/off	$V_T [\text{V}]$
P4TIF	0.34 ± 0.033	$> 10^4$	-10.3 ± 2.0
P4TIH	0.20 ± 0.011	$> 10^4$	-6.8 ± 1.1
P4TIN	0.18 ± 0.005	$> 10^4$	-18.9 ± 4.1

Table S4. Electrical properties of P4TIF-HV_TA films.

Sample	$\mu_{\text{sat}} [\text{cm}^2\text{V}^{-1}\text{s}^{-1}]$	on/off	$V_T [\text{V}]$
P4F-100%_TA	0.34 ± 0.033	$> 10^4$	-10.3 ± 2.0
P4F-80%_TA	0.32 ± 0.049	$> 10^4$	-14.3 ± 1.8
P4F-75%_TA	0.30 ± 0.064	$> 10^4$	-10.3 ± 0.8
P4F-67%_TA	0.32 ± 0.053	$> 10^4$	-10.0 ± 1.2
P4F-50%_TA	0.39 ± 0.050	$> 10^4$	-14.0 ± 2.7
P4F-33%_TA	0.19 ± 0.043	$> 10^3$	-14.6 ± 1.7

Table S5. Electrical properties of P4TIF-HV_w films.

Sample	$\mu_{\text{sat}} [\text{cm}^2\text{V}^{-1}\text{s}^{-1}]$	on/off	$V_T [\text{V}]$
P4F-80%_w	0.052 ± 0.003	$> 10^3$	-8.0 ± 1.0
P4F-75%_w	0.052 ± 0.001	$> 10^3$	-5.6 ± 0.2
P4F-67%_w	0.053 ± 0.002	$> 10^3$	-11.6 ± 0.2
P4F-50%_w	0.071 ± 0.004	$> 10^3$	-8.3 ± 0.4
P4F-33%_w	0.055 ± 0.004	$> 10^3$	-11.0 ± 1.0

Table S6. Electrical properties of P4TIF-HV_ac films.

Sample	μ_{sat} [cm ² V ⁻¹ s ⁻¹]	on/off	V _T [V]
P4F-100%_ac	0.071 ± 0.020	> 10 ³	-32.1 ± 6.9
P4F-80%_ac	0.030 ± 0.001	> 10 ³	-29.0 ± 3.1
P4F-75%_ac	0.030 ± 0.003	> 10 ³	-32.3 ± 5.1
P4F-67%_ac	0.026 ± 0.002	> 10 ³	-40.4 ± 3.3
P4F-50%_ac	0.037 ± 0.003	> 10 ³	-39.6 ± 3.6
P4F-33%_ac	0.038 ± 0.002	> 10 ³	-43.9 ± 3.8